CHAPTER 6

SAR Automatic Target Recognition using FCOM Texture Features

Synthetic Aperture Radar (SAR) Automatic Target Recognition (ATR) using FCOM texture feature is reported [54]. The difficulty of this problem is the difference between SAR images and their optical images. Experiments were tested on MSTAR public release data set [55]. We also compared the results with the feature sets extracted from GLCM. Moreover, we implemented an ensemble average [56] to improve the recognition rates. This chapter is organized in three sections. Section 6.1 describes the experimental design. The recognition results of SAR-ATR are shown in section 6.2. Finally, SAR target recognition summary and discussion are given in section 6.3.

6.1 Experimental design

According to the previous chapters, we generated the two groups of feature sets from FCOM and GLCM. In the experiment, *d*, the distance of pixel pair is varied among 1, 2, 3, 5, and 10. We varied the number of clusters, *C*, for FCM among 2, 3, 4, 5, 6, 7, 8, 16, and 32 to compute the FCOM. Similar to FCOM, we varied the number of gray levels, N_g, for GLCM equal to the number of clusters. The texture extraction detail of these feature sets are shown in table 6.1. The dimensions of GLCM feature sets were 4, 16, 8, 14, 56, and 28, respectively, while the dimensions of FCOM feature sets are shown in table 6.2. To reduce the correlation of features, each feature was normalized using (4.1).

Therefore, another classifier used in this experiment was the RBF network [57]. The output of node *i* in the hidden layer is not calculated from the inner product between input vector **x** with weights, but instead it is calculated from

$$y_i = \exp\left(\frac{-\|x - t_i\|^2}{(\sigma / 0.8326)^2} \right) \tag{6.1}$$

where $\mathbf{t}_i$ is the center of node i and σ is the spread of node i. The output of node j in the output layer will be the inner product between inputs coming to node j with their weights. The linear least square method [58] is implemented for the weights training.

To improve the result, we implemented the ensemble average, the simple fusion method, by averaging the output from all the outputs. We only used $D_i(\mathbf{x})$ for i = 1, 2, and 3 to fuse the output from multi-class SVM and then computed the average of those values over the M best MSVM models by

$$F_i(\mathbf{x}) = \frac{1}{M}\sum_{j=1}^{M} D_i^j(\mathbf{x}) \tag{6.2}$$

where $D_i^j(\mathbf{x})$ is the discriminant function of class i from model j for input vector $\mathbf{x}$, and $F_i(\mathbf{x})$ is the fused output of class i for input vector $\mathbf{x}$. We also implemented a similar scheme for the fusion of the M best RBF network models. The proposed SAR automatic target recognition workflow is shown in figure 6.1.

We set the same parameters for both MSVM and RBF network. That was σ = 0.01, 0.25, 0.50, 0.75, and 1 to 50 with the step size of 0.5. For the RBF network, we let the number of hidden nodes equal to the number of training feature vectors and use those feature vectors to be the centers of hidden nodes. We also implemented 10-fold cross validation for the generalized system in training process.

Table 6.1 FCOM and GLCM feature sets.

Name		**θ Combination**	**Feature**
FCOM	**GLCM**		
FzCM1	GLCM1	0°	f_1 - f_4
FzCM2	GLCM2	0°, 45°, 90°, and 135°	f_1 - f_4
FzCM3	GLCM3	0°, 45°, 90°, and 135°	μ_{f1} - μ_{f4}, σ_{f1} - σ_{f4}
FzCM4	GLCM4	0°	f_1 - f_{14}
FzCM5	GLCM5	0°, 45°, 90°, and 135°	f_1 - f_{14}
FzCM6	GLCM6	0°, 45°, 90°, and 135°	μ_{f1} - μ_{f14}, σ_{f1} - σ_{f14}

Table 6.2 Dimensions of FCOM feature sets.

C	No. of feature dimensions					
	FzCM1	FzCM2	FzCM3	FzCM4	FzCM5	FzCM6
2	8	32	16	28	112	56
3	12	48	24	42	168	84
4	16	64	32	56	224	112
5	20	80	40	70	280	140
6	24	96	48	84	336	168
7	28	112	56	98	392	196
8	32	128	64	112	448	224
16	64	256	128	224	896	448
32	128	512	256	448	1792	896

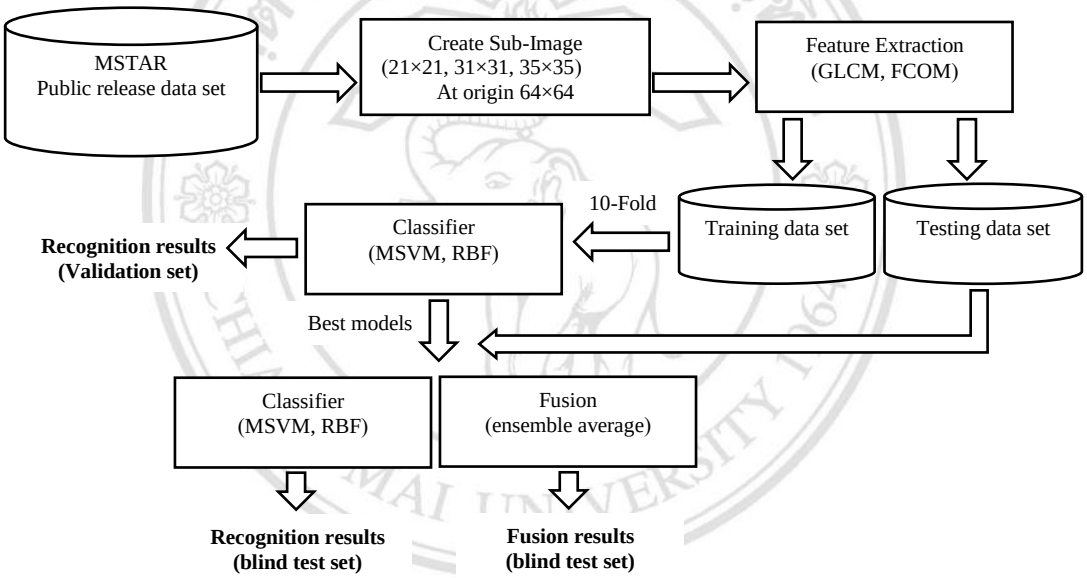

Figure 6.1 System workflow for SAR automatic target recognition.

6.2 Recognition results and discussions

The experiments were tested on the MSTAR public data set which was collected by the DARPA/WRIGHT laboratory Moving and Stationary Acquisition and Recognition (MSTAR) program. The data set consists of three different tanks and three armored personnel carriers (APCs) defined by their serial numbers. In this study, we selected only T72 tank with serial number S7, BMP2 APCs with serial number C21, and BTR70 APCs with serial number C71. They were totally 1277 images with the size of 128×128 pixels used in training and testing processes where we showed their details in table 6.3.

Since the object was assumed to be at the center of each SAR image, we used a square window of size $N \times N$ centered at (64, 64) to extract the features. We varied N to 21, 31, and 35 in this experiment. The examples of objects in each window size are shown in table 6.4 where we also zoomed in some images for the display purpose in this figure.

Table 6.3 MSTAR data set.

Vehicle Type	Training data set	Testing data set	Total images
BMP2	233	196	429
BTR70	233	196	429
T72	228	191	419
Total images	694	583	1277

Table 6.4 Examples of SAR image objects in different window sizes.

Vehicle Type	Optical image	SAR images (128×128)	Sub-images		
			21×21	31×31	35×35
BMP2		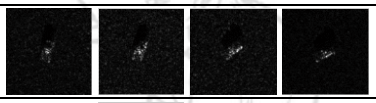	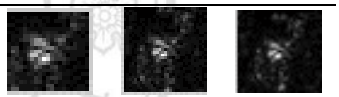		
BTR70		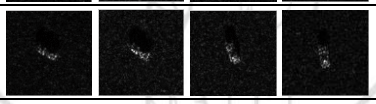	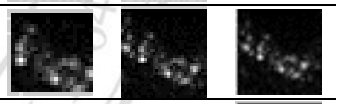		
T72		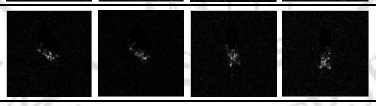	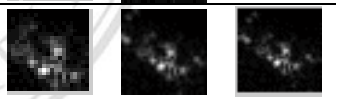		

The classification results from FCOM feature sets with SVM classifier were 97.14% and 85.59% for validation set and blind test set, respectively, while the best classification results with RBF network were 98.55% and 89.02%, respectively. The classification results with different FCOM distant are shown in figure 6.2. The details of recognition results from FCOM feature sets are shown in table 6.5. The confusion matrices of the recognition results from table 6.5 are shown in table 6.6 to 6.15, respectively.

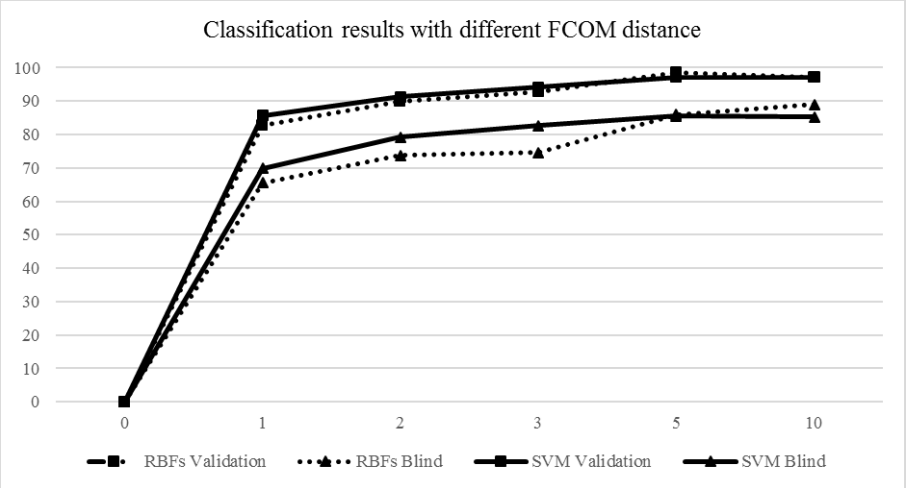

Figure 6.2 Classification results with different FCOM distance.

Table 6.5 The best classification rates using FCOM for d = 1, 2, 3, 5, and 10.

d	MSVM						RBF network					
	C	N	RBF σ	Feature set	Validation	Blind test set	C	N	σ	Feature set	Validation	Blind
1	32	35	24.50	FzCM5	85.71	69.81	7	35	30.00	FzCM5	82.61	65.52
2	16	35	11.00	FzCM2	91.30	79.25	6	35	11.50	FzCM5	90.00	73.76
3	7	35	8.50	FzCM5	94.20	82.68	7	35	7.50	FzCM2	92.86	74.61
5	8	35	10.50	FzCM5	97.14	85.59	16	31	22.50	FzCM5	98.55	85.93
10	7	31	7.00	FzCM2	97.14	85.25	6	35	33.00	FzCM5	97.14	89.02

Table 6.6 Confusion matrices of the results in table 6.5 from MSVM for d = 1.

Validation set

Actual \ Algorithm	BMP2	BTR70	T72
BMP2	19	3	2
BTR70	2	20	1
T72	2	0	21

Blind test set

Actual \ Algorithm	BMP2	BTR70	T72
BMP2	135	20	41
BTR70	51	108	37
T72	10	17	164

Table 6.7 Confusion matrices of the results in table 6.5 from MSVM for d = 2.

Validation set

Actual \ Algorithm	BMP2	BTR70	T72
BMP2	21	0	2
BTR70	3	19	1
T72	0	0	23

Blind test set

Actual \ Algorithm	BMP2	BTR70	T72
BMP2	144	18	34
BTR70	24	152	20
T72	12	13	166

Table 6.8 Confusion matrices of the results in table 6.5 from MSVM for $d = 3$.

Validation set

Actual \ Algorithm	BMP2	BTR70	T72
BMP2	21	2	0
BTR70	1	22	0
T72	0	1	22

Blind test set

Actual \ Algorithm	BMP2	BTR70	T72
BMP2	152	19	25
BTR70	22	153	21
T72	6	8	177

Table 6.9 Confusion matrices of the results in table 6.5 from MSVM for $d = 5$.

Validation set

Actual \ Algorithm	BMP2	BTR70	T72
BMP2	24	0	0
BTR70	1	22	0
T72	1	0	22

Blind test set

Actual \ Algorithm	BMP2	BTR70	T72
BMP2	152	14	30
BTR70	18	171	7
T72	5	10	176

Table 6.10 Confusion matrices of the results in table 6.5 from MSVM for $d = 10$.

Validation set

Actual \ Algorithm	BMP2	BTR70	T72
BMP2	22	1	0
BTR70	1	23	0
T72	0	0	23

Blind test set

Actual \ Algorithm	BMP2	BTR70	T72
BMP2	150	18	28
BTR70	19	172	5
T72	11	5	175

Table 6.11 Confusion matrices of the results in table 6.5 from RBF network for $d = 1$.

Validation set

Actual \ Algorithm	BMP2	BTR70	T72
BMP2	19	4	0
BTR70	4	17	2
T72	1	1	21

Blind test set

Actual \ Algorithm	BMP2	BTR70	T72
BMP2	129	25	42
BTR70	47	119	30
T72	33	24	134

Table 6.12 Confusion matrices of the results in table 6.5 from RBF network for $d = 2$.

Validation set

Actual \ Algorithm	BMP2	BTR70	T72
BMP2	19	3	2
BTR70	0	22	1
T72	0	1	22

Blind test set

Actual \ Algorithm	BMP2	BTR70	T72
BMP2	112	54	30
BTR70	32	158	6
T72	12	19	160

Table 6.13 Confusion matrices of the results in table 6.5 from RBF network for $d = 3$.

Validation set

Actual \ Algorithm	BMP2	BTR70	T72
BMP2	21	1	2
BTR70	0	23	0
T72	1	1	21

Blind test set

Actual \ Algorithm	BMP2	BTR70	T72
BMP2	111	25	60
BTR70	27	150	19
T72	9	8	174

Table 6.14 Confusion matrices of the results in table 6.5 from RBF network for $d = 5$.

Validation set

Actual \ Algorithm	BMP2	BTR70	T72
BMP2	22	1	0
BTR70	0	24	0
T72	0	0	22

Blind test set

Actual \ Algorithm	BMP2	BTR70	T72
BMP2	153	21	22
BTR70	20	169	7
T72	6	6	179

Table 6.15 Confusion matrices of the results in table 6.5 from RBF network for $d = 10$.

Validation set

Actual \ Algorithm	BMP2	BTR70	T72
BMP2	21	2	0
BTR70	0	24	0
T72	0	0	23

Blind test set

Actual \ Algorithm	BMP2	BTR70	T72
BMP2	159	16	21
BTR70	7	187	2
T72	13	5	173

For the GLCM feature sets, the best classification results with SVM classifier were 92.75% and 79.59% at the same training and testing data sets of FCOM, respectively, whereas the best classification results with RBF network were 92.86% and 82.50%, respectively. The classification results with different GLCM distant are shown in figure 6.3. The details of recognition results from GLCM feature sets are shown in table 6.16. The confusion matrices of the recognition results from table 6.16 are shown in table 6.17 to 6.26, respectively.

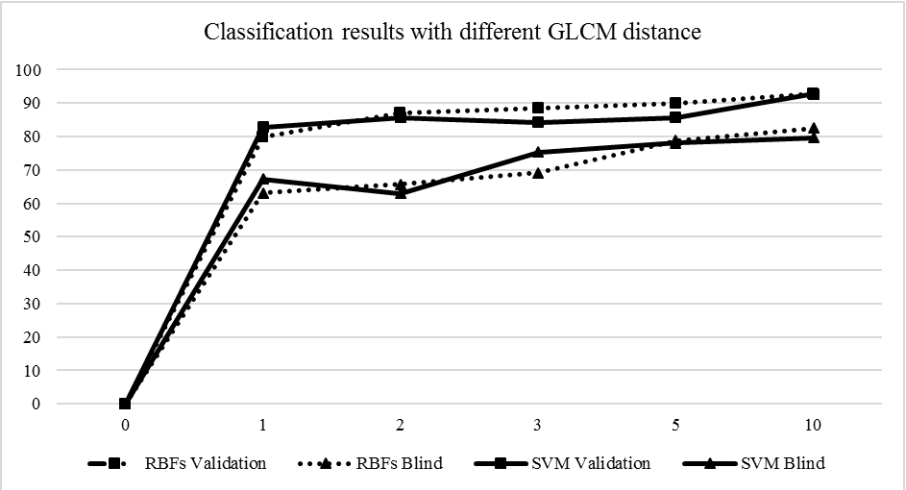

Figure 6.3 Classification results with different GLCM distance.

Table 6.16 The best classification rates using GLCM for d = 1, 2, 3, 5, and 10.

d	MSVM						RBF network					
	N_g	N	RBF σ	Feature set	Validation	Blind test set	N_g	N	σ	Feature set	Validation	Blind
1	32	31	3.00	GLCM6	82.89	67.24	32	35	2.50	GLCM6	79.71	63.12
2	32	31	2.50	GLCM5	85.71	62.95	32	31	23.50	GLCM5	87.14	65.69
3	32	31	2.50	GLCM6	84.29	75.30	32	35	9.50	GLCM5	88.41	69.13
5	32	35	2.50	GLCM6	85.71	78.04	32	35	16.50	GLCM5	89.86	78.73
10	32	21	2.50	GLCM5	92.75	79.59	32	35	23.50	GLCM5	92.86	82.50

Table 6.17 Confusion matrices of the results in table 6.16 from MSVM for d = 1.

Validation set

Actual \ Algorithm	BMP2	BTR70	T72
BMP2	19	1	3
BTR70	3	17	4
T72	0	1	22

Blind test set

Actual \ Algorithm	BMP2	BTR70	T72
BMP2	125	32	39
BTR70	56	110	30
T72	18	16	157

Table 6.18 Confusion matrices of the results in table 6.16 from MSVM for d = 2.

Validation set

Actual \ Algorithm	BMP2	BTR70	T72
BMP2	18	3	3
BTR70	0	21	2
T72	1	1	21

Blind test set

Actual \ Algorithm	BMP2	BTR70	T72
BMP2	96	49	51
BTR70	36	126	34
T72	25	21	145

Table 6.19 Confusion matrices of the results in table 6.16 from MSVM for $d = 3$.

Validation set

Actual \ Algorithm	BMP2	BTR70	T72
BMP2	21	2	1
BTR70	4	17	2
T72	1	1	21

Blind test set

Actual \ Algorithm	BMP2	BTR70	T72
BMP2	132	29	35
BTR70	27	151	18
T72	22	13	156

Table 6.20 Confusion matrices of the results in table 6.16 from MSVM for $d = 5$.

Validation set

Actual \ Algorithm	BMP2	BTR70	T72
BMP2	19	5	0
BTR70	4	18	1
T72	0	0	23

Blind test set

Actual \ Algorithm	BMP2	BTR70	T72
BMP2	143	20	33
BTR70	27	153	16
T72	14	18	159

Table 6.21 Confusion matrices of the results in table 6.16 from MSVM for $d = 10$.

Validation set

Actual \ Algorithm	BMP2	BTR70	T72
BMP2	20	1	2
BTR70	0	22	1
T72	1	0	22

Blind test set

Actual \ Algorithm	BMP2	BTR70	T72
BMP2	139	33	24
BTR70	25	158	13
T72	17	7	167

Table 6.22 Confusion matrices of the results in table 6.16 from RBF network for $d = 1$.

Validation set

Actual \ Algorithm	BMP2	BTR70	T72
BMP2	16	3	4
BTR70	4	18	1
T72	0	2	21

Blind test set

Actual \ Algorithm	BMP2	BTR70	T72
BMP2	118	43	35
BTR70	52	116	28
T72	19	38	134

Table 6.23 Confusion matrices of the results in table 6.16 from RBF network for $d = 2$.

Validation set

Actual \ Algorithm	BMP2	BTR70	T72
BMP2	23	1	0
BTR70	4	18	1
T72	3	0	20

Blind test set

Actual \ Algorithm	BMP2	BTR70	T72
BMP2	130	21	45
BTR70	46	116	34
T72	36	18	137

Table 6.24 Confusion matrices of the results in table 6.16 from RBF network for $d = 3$.

Validation set

Actual \ Algorithm	BMP2	BTR70	T72
BMP2	18	4	1
BTR70	1	20	2
T72	0	0	23

Blind test set

Actual \ Algorithm	BMP2	BTR70	T72
BMP2	109	51	36
BTR70	33	144	19
T72	17	24	150

Table 6.25 Confusion matrices of the results in table 6.16 from RBF network for $d = 5$.

Validation set

Actual \ Algorithm	BMP2	BTR70	T72
BMP2	20	2	1
BTR70	0	21	2
T72	1	1	21

Blind test set

Actual \ Algorithm	BMP2	BTR70	T72
BMP2	155	19	22
BTR70	27	158	11
T72	23	22	146

Table 6.26 Confusion matrices of the results in table 6.16 from RBF network for $d = 10$.

Validation set

Actual \ Algorithm	BMP2	BTR70	T72
BMP2	22	0	2
BTR70	3	20	0
T72	0	0	23

Blind test set

Actual \ Algorithm	BMP2	BTR70	T72
BMP2	155	19	22
BTR70	18	159	19
T72	14	10	167

For the fusion method, three schemes of ensemble average were studied. The first fusion results were from the outputs of the ten best validation MSVM models and ten best validation RBF network models. This fusion scheme is shown in figure 6.4. We selected the best models from the 10 best models at different FCOM feature sets, different N, and different σ. Table 6.27 shows the ten best models fusion results using FCOM feature sets. The confusion matrices of ensemble average in table 6.27 are shown in table 6.28 to 6.32.

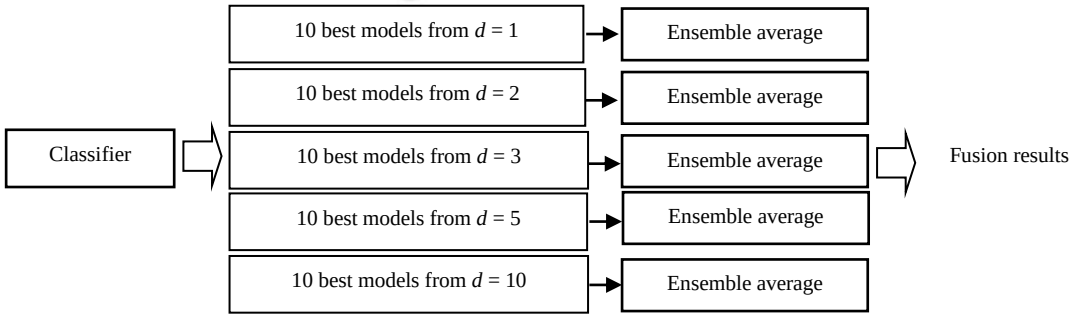

Figure 6.4 The first fusion scheme used in this experiment.

Table 6.27 Ensemble average fusion results from the 10 best models using FCOM at d = 1, 2, 3, 5, and 10.

d	MSVM (%)			RBFs (%)		
	Validation	Blind	Ensemble 10 best models	Validation	Blind	Ensemble 10 best models
1	85.71	69.81	70.33	82.61	65.52	72.56
2	91.30	79.25	83.53	90.00	73.76	85.08
3	94.20	82.68	87.31	92.86	74.61	88.16
5	97.14	85.59	89.19	98.55	85.93	92.80
10	97.14	85.25	93.14	97.14	89.02	96.23

Table 6.28 Confusion matrices of the results in table 6.27 for d = 1.

MSVM

Actual \ Algorithm	BMP2	BTR70	T72
BMP2	142	14	40
BTR70	55	96	45
T72	13	6	172

RBF network

Actual \ Algorithm	BMP2	BTR70	T72
BMP2	141	22	33
BTR70	51	123	22
T72	18	14	159

Table 6.29 Confusion matrices of the results in table 6.27 for d = 2.

MSVM

Actual \ Algorithm	BMP2	BTR70	T72
BMP2	156	15	25
BTR70	26	158	12
T72	11	7	173

RBF network

Actual \ Algorithm	BMP2	BTR70	T72
BMP2	151	29	16
BTR70	18	172	6
T72	6	12	173

Table 6.30 Confusion matrices of the results in table 6.27 for d = 3.

MSVM

Actual \ Algorithm	BMP2	BTR70	T72
BMP2	161	11	24
BTR70	20	167	9
T72	8	2	181

RBF network

Actual \ Algorithm	BMP2	BTR70	T72
BMP2	157	19	20
BTR70	12	177	7
T72	5	6	180

Table 6.31 Confusion matrices of the results in table 6.27 for d = 5.

MSVM

Actual \ Algorithm	BMP2	BTR70	T72
BMP2	162	10	24
BTR70	13	177	6
T72	4	6	181

RBF network

Actual \ Algorithm	BMP2	BTR70	T72
BMP2	171	8	17
BTR70	6	186	4
T72	3	4	184

Table 6.32 Confusion matrices of the results in table 6.27 for $d = 10$.

MSVM

Actual \ Algorithm	BMP2	BTR70	T72
BMP2	173	7	16
BTR70	7	186	3
T72	5	2	184

RBF network

Actual \ Algorithm	BMP2	BTR70	T72
BMP2	182	1	13
BTR70	2	192	2
T72	4	0	187

We also implemented this fusion scheme using feature sets from GLCM. The ten best models from different GLCM feature sets, different *N*, and different σ were selected. Table 6.33 shows the ten best models fusion results using FCOM feature sets. The confusion matrices of ensemble average in table 6.33 are shown in table 6.34 to 6.38.

Table 6.33 Ensemble average fusion results from the 10 best models using GLCM at $d = 1, 2, 3, 5$, and 10.

d	MSVM (%)			RBFs (%)		
	Validation	Blind	Ensemble 10 best models	Validation	Blind	Ensemble 10 best models
1	82.86	67.24	68.27	79.71	63.12	75.81
2	85.71	62.95	72.21	87.14	65.69	77.70
3	84.29	75.30	80.45	88.41	69.13	83.71
5	85.71	78.04	84.39	89.86	78.73	89.02
10	92.75	79.59	85.25	92.86	82.50	92.80

Table 6.34 Confusion matrices of the results in table 6.33 for $d = 1$.

MSVM

Actual \ Algorithm	BMP2	BTR70	T72
BMP2	124	32	40
BTR70	46	115	35
T72	23	9	159

RBF network

Actual \ Algorithm	BMP2	BTR70	T72
BMP2	143	33	20
BTR70	39	141	16
T72	17	16	158

Table 6.35 Confusion matrices of the results in table 6.33 for $d = 2$.

MSVM

Actual \ Algorithm	BMP2	BTR70	T72
BMP2	135	36	25
BTR70	39	135	22
T72	22	18	151

RBF network

Actual \ Algorithm	BMP2	BTR70	T72
BMP2	134	38	24
BTR70	23	161	12
T72	19	14	158

Table 6.36 Confusion matrices of the results in table 6.33 for $d = 3$.

MSVM

Actual \ Algorithm	BMP2	BTR70	T72
BMP2	139	35	22
BTR70	21	168	8
T72	20	8	163

RBF network

Actual \ Algorithm	BMP2	BTR70	T72
BMP2	155	25	16
BTR70	21	166	9
T72	12	12	167

Table 6.37 Confusion matrices of the results in table 6.33 for $d = 5$.

MSVM

Actual \ Algorithm	BMP2	BTR70	T72
BMP2	148	29	19
BTR70	10	178	8
T72	15	10	166

RBF network

Actual \ Algorithm	BMP2	BTR70	T72
BMP2	171	9	16
BTR70	18	174	4
T72	11	6	174

Table 6.38 Confusion matrices of the results in table 6.33 for $d = 10$.

MSVM

Actual \ Algorithm	BMP2	BTR70	T72
BMP2	151	25	20
BTR70	14	177	5
T72	13	9	169

RBF network

Actual \ Algorithm	BMP2	BTR70	T72
BMP2	171	14	11
BTR70	6	189	1
T72	9	1	181

From the fusion results from the first fusion scheme, we found that the results from FCOM gave better results than the results from GLCM in any cases. The confusion matrices showed that the incorrect recognition were almost from the same vehicle types, i.e., BMP2 classified as BTR70 and BTR70 classified as BMP2. The reason in this case was the characteristics of itself. The APCs shape was thin and long while the tank shape was wide and short.

For the second fusion scheme, we selected the best models from the output of 1 - 10 best validation MSVM models and 1 - 10 best validation RBF network models. This best models were selected from different feature sets, different d, different N, and different σ. This fusion scheme is shown in figure 6.5. The best correct recognition results using FCOM feature sets were 95.37% and 97.94% for MSVM and RBF network classifiers, respectively. Both of them were from the 10 best models at d = 5 and 10. Table 6.39 shows the fusion results of this fusion framework using FCOM

feature sets. The confusion matrices of ensemble average in table 6.39 are shown in table 6.40 to 6.43.

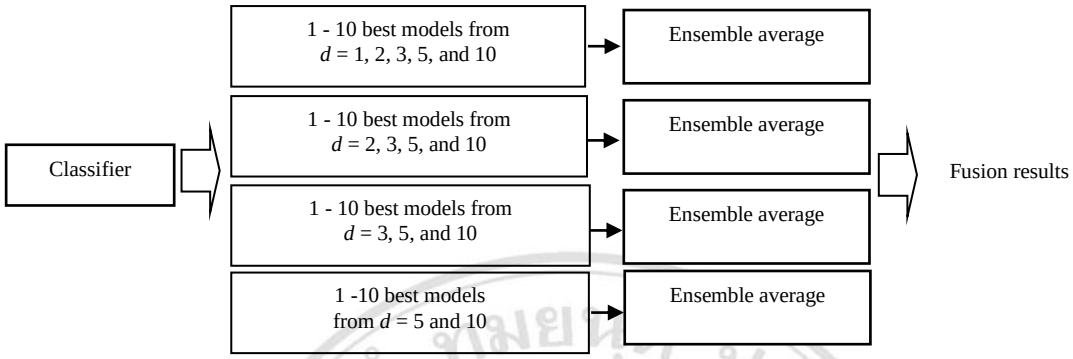

Figure 6.5 The second fusion scheme used in this experiment.

Table 6.39 Ensemble average fusion results from the *M* best models using FCOM at different feature sets, different *d*, different *N*, and different σ.

No. of best models	*d* = 1, 2, 3, 5, and 10		*d* = 2, 3, 5, and 10		*d* = 3, 5, and 10		*d* = 5 and 10	
	MSVM	RBF network	MSVM	RBF network	MSVM	RBF network	MSVM	RBF network
1	92.45	89.54	93.65	89.02	91.94	91.94	92.11	93.31
2	90.91	91.77	92.80	92.78	92.45	93.65	92.45	95.37
3	91.08	92.45	92.97	92.98	94.00	94.34	94.00	96.05
4	91.77	92.62	92.97	94.68	94.51	94.68	95.03	97.26
5	91.60	92.80	93.14	94.85	94.34	95.03	94.85	97.26
6	91.60	94.00	92.97	95.54	94.34	95.71	95.37	97.08
7	91.25	94.51	93.14	95.54	94.51	96.40	95.03	97.08
8	91.94	94.85	93.31	96.57	94.34	96.74	95.03	97.26
9	91.77	94.68	93.65	96.57	94.51	96.91	94.68	97.77
10	92.11	94.85	93.65	96.74	95.03	97.43	95.37	97.94

Table 6.40 Confusion matrices of the best results in table 6.39 for *d* = 1, 2, 3, 5, and 10.

MSVM

Actual \ Algorithm	BMP2	BTR70	T72
BMP2	171	5	20
BTR70	10	184	2
T72	5	2	184

RBF network

Actual \ Algorithm	BMP2	BTR70	T72
BMP2	178	9	9
BTR70	5	190	1
T72	5	1	185

Table 6.41 Confusion matrices of the best results in table 6.39 for d = 2, 3, 5, and 10.

MSVM

Actual \ Algorithm	BMP2	BTR70	T72
BMP2	173	3	20
BTR70	7	188	1
T72	5	1	185

RBF network

Actual \ Algorithm	BMP2	BTR70	T72
BMP2	184	6	6
BTR70	1	195	0
T72	4	2	185

Table 6.42 Confusion matrices of the best results in table 6.39 for d = 3, 5, and 10.

MSVM

Actual \ Algorithm	BMP2	BTR70	T72
BMP2	177	4	15
BTR70	4	191	1
T72	5	0	186

RBF network

Actual \ Algorithm	BMP2	BTR70	T72
BMP2	185	2	9
BTR70	0	196	0
T72	4	0	187

Table 6.43 Confusion matrices of the best results in table 6.39 for d = 5 and 10.

MSVM

Actual \ Algorithm	BMP2	BTR70	T72
BMP2	178	5	13
BTR70	3	192	1
T72	5	0	186

RBF network

Actual \ Algorithm	BMP2	BTR70	T72
BMP2	189	2	5
BTR70	0	195	1
T72	4	0	187

We also implemented this fusion scheme using feature sets from GLCM. The best incorrect recognition results were 88.16% at d = 5 and 10 with 6 best models, and 100% at d = 3, 5, and 10 with 9 best models for MSVM and RBF network, respectively. Table 6.44 shows the ten best models fusion results using FCOM feature sets. The confusion matrices of ensemble average in table 6.44 are shown in table 6.45 to 6.48.

Table 6.44 Ensemble average fusion results from the M best models using GLCM at different feature sets, different d, different N, and different σ.

No. of best models	d = 1, 2, 3, 5, and 10		d = 2, 3, 5, and 10		d = 3, 5, and 10		d = 5 and 10	
	MSVM	RBF network	MSVM	RBF network	MSVM	RBF network	MSVM	RBF network
1	83.70	89.02	83.53	88.16	83.88	88.34	87.14	89.02
2	85.59	91.08	85.76	92.28	86.62	92.45	86.28	90.05
3	85.08	93.31	86.28	92.97	86.96	94.34	85.93	93.83
4	85.25	93.48	86.11	93.83	87.14	95.03	87.65	95.20
5	85.25	93.31	85.42	94.00	86.62	95.88	87.82	95.54
6	85.08	92.80	85.76	93.14	87.31	95.37	88.16	94.51

7	84.22	92.62	84.73	92.80	87.31	94.85	87.14	95.37
8	84.73	93.14	84.91	93.48	87.14	94.85	86.96	95.20
9	85.42	92.80	85.59	93.14	87.14	96.23	87.31	95.20
10	85.08	93.31	85.59	93.14	86.79	95.88	87.31	94.68

Table 6.45 Confusion matrices of the best results in table 6.44 for $d = 1$, 2, 3, 5, and 10.

MSVM

Actual \ Algorithm	BMP2	BTR70	T72
BMP2	152	23	21
BTR70	14	171	11
T72	10	5	176

RBF network

Actual \ Algorithm	BMP2	BTR70	T72
BMP2	176	10	10
BTR70	10	182	4
T72	2	2	187

Table 6.46 Confusion matrices of the best results in table 6.44 for $d = 2$, 3, 5, and 10.

MSVM

Actual \ Algorithm	BMP2	BTR70	T72
BMP2	154	19	23
BTR70	15	174	7
T72	9	7	175

RBF network

Actual \ Algorithm	BMP2	BTR70	T72
BMP2	179	10	7
BTR70	11	183	2
T72	3	2	186

Table 6.47 Confusion matrices of the best results in table 6.44 for $d = 3$, 5, and 10.

MSVM

Actual \ Algorithm	BMP2	BTR70	T72
BMP2	155	23	18
BTR70	11	179	6
T72	11	5	175

RBF network

Actual \ Algorithm	BMP2	BTR70	T72
BMP2	186	8	2
BTR70	5	191	0
T72	3	4	184

Table 6.48 Confusion matrices of the best results in table 6.44 for $d = 5$ and 10.

MSVM

Actual \ Algorithm	BMP2	BTR70	T72
BMP2	158	18	20
BTR70	7	183	6
T72	13	5	173

RBF network

Actual \ Algorithm	BMP2	BTR70	T72
BMP2	185	5	6
BTR70	6	186	4
T72	4	1	186

From the results of the second fusion framework, we found that the best correct recognition rates were better than those from the first fusion framework because we select the best models from a different *d*. The feature set extracted from different distant provided more information than the feature set extracted from the same distant. Again, the best classification result in this case was from the FCOM feature set as 97.74%.

For the last fusion scheme, we fused the output from MSVM and RBF network together. The best models from the output of 1 - 10 best validation MSVM models and 1 - 10 best validation RBF network models were selected. These best models were selected from different feature sets, different *d*, different *N*, and different σ. This fusion scheme is shown in figure 6.6. The best correct recognition results using FCOM feature sets was 97.08% at *d* = 5 and 10 with the 10 best models from MSVM and the other 10 best models from RBF network. The best correct recognition results using GLCM feature sets was 93.83% at *d* = 5 and 10 with the 4 best models from MSVM and the other 4 best models from RBF network. Table 6.49 shows the fusion results of this fusion framework using FCOM feature sets. The confusion matrices of ensemble average in table 6.49 are shown in table 6.50 to 6.53.

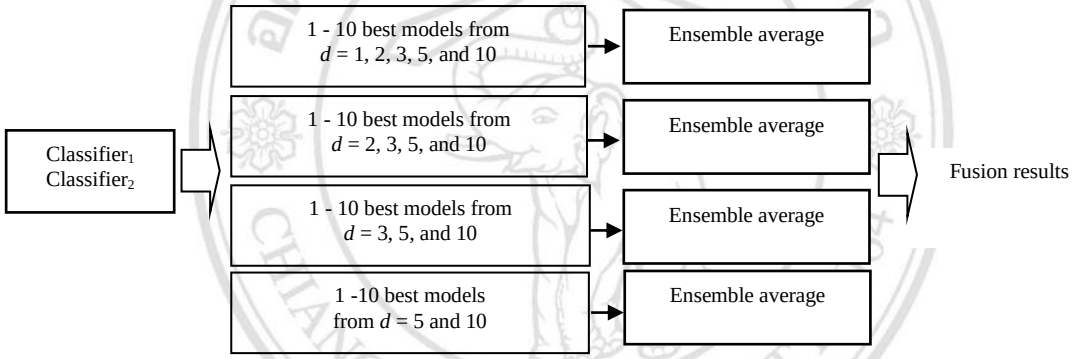

Figure 6.6 The third fusion scheme used in this experiment.

Table 6.49 MSVM and RBF network ensemble average fusion results from the *M* best models at different feature sets, different *d*, different *N*, and different σ.

Method	Distant	No. of best models									
		1	2	3	4	5	6	7	8	9	10
FCOM	d = 1,2,3,5, and 10	91.60	92.80	92.28	92.80	92.45	92.62	93.14	93.48	93.65	93.31
	d = 2,3,5, and 10	92.45	92.97	92.97	94.00	94.34	94.51	94.34	94.51	94.68	94.68
	d = 3,5, and 10	93.48	93.83	93.83	94.34	94.85	95.37	95.71	96.05	96.23	96.23
	d = 5 and 10	94.34	95.03	96.05	96.74	96.40	96.91	96.57	97.08	96.91	97.08
GLCM	d = 1,2,3,5, and 10	89.37	90.57	91.60	91.77	89.54	89.54	89.71	90.22	90.74	90.74
	d = 2,3,5, and 10	91.25	91.42	91.42	92.8	92.11	91.08	91.94	91.42	91.08	91.77
	d = 3,5, and 10	92.45	92.97	92.62	92.97	93.83	92.97	93.31	92.45	92.45	92.45
	d = 5 and 10	91.94	92.97	93.14	93.83	93.65	93.31	93.48	92.62	92.11	92.11

Table 6.50 Confusion matrices of the best results in table 6.49 for $d = 1$, 2, 3, 5, and 10.

FCOM

Actual \ Algorithm	BMP2	BTR70	T72
BMP2	174	4	18
BTR70	7	188	1
T72	6	1	184

GLCM

Actual \ Algorithm	BMP2	BTR70	T72
BMP2	172	12	12
BTR70	13	178	5
T72	6	0	185

Table 6.51 Confusion matrices of the best results in table 6.49 for $d = 2$, 3, 5, and 10.

FCOM

Actual \ Algorithm	BMP2	BTR70	T72
BMP2	178	3	15
BTR70	5	190	1
T72	6	1	184

GLCM

Actual \ Algorithm	BMP2	BTR70	T72
BMP2	175	11	10
BTR70	10	181	5
T72	4	2	185

Table 6.52 Confusion matrices of the best results in table 6.49 for $d = 3$, 5, and 10.

FCOM

Actual \ Algorithm	BMP2	BTR70	T72
BMP2	181	4	11
BTR70	2	193	1
T72	4	0	187

GLCM

Actual \ Algorithm	BMP2	BTR70	T72
BMP2	181	10	5
BTR70	9	183	4
T72	6	2	183

Table 6.53 Confusion matrices of the best results in table 6.49 for $d = 5$, and 10.

FCOM

Actual \ Algorithm	BMP2	BTR70	T72
BMP2	183	4	9
BTR70	1	195	0
T72	3	0	188

GLCM

Actual \ Algorithm	BMP2	BTR70	T72
BMP2	178	9	9
BTR70	8	185	3
T72	6	1	184

From the results of the last fusion framework, we found that the best correct recognition rates are similar to those from the second fusion framework because we selected the best models from a different classifier and different *d*. The factor of the classification fusion results in this case was a characteristic of the classifier. The classifier who gives the best recognition results can also give the best fusion results also. Again, the best classification result in this case was from the FCOM feature set as 97.08% increasing from the GLCM feature set up to 3.25%.

6.3 Summary

In this chapter, the synthetic aperture radar (SAR) image classification using the texture features computed from the FCOM and GLCM was reported. We implemented these features on the MSVM and the RBF network. We also utilized the ensemble average as an information fusion tool. This fusion technique was applied to the outputs from each classifier in each distance *d*, and the outputs from several best models from several *d* of each classifier. The summarized of the best recognition results from the experiments is shown in table 6.54. We concluded that the detection results from FCOM have been better than that from GLCM in any cases.

Table 6.54 Summarized of the best MSTAR SAR detection results.

Detection result	Classifier	Fusion models	Feature set
97.94%	RBF network	10 models at d = 5, 10 models at d = 10	FCOM
95.37%	MSVM	10 models at d = 5, 10 models at d = 10	FCOM

From all the detection results, we concluded that FCOM performs better than GLCM in all the case in the experiment. With the same setting parameters, the FCOM plane has more information than the GLCM plane. Hence, the FCOM plane was equal to the number of clusters mentioned in chapter 3 whereas there was only one GLCM plane. An original BMP2 SAR image and its corresponding sub-image (N = 35) are shown in figure 6.7 (a) and (b). The corresponding GLCM and FCOM planes with C = 8, θ = 0°, and d = 1, 2, 3, 5, and 10 of figure 6.5 (b) are shown in figure 6.7 (c) to 6.7 (l), respectively. The FCOM planes were more information provided with larger d while the GLCM planes were similar for all d.

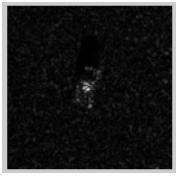

(a) Original BMP2 SAR image

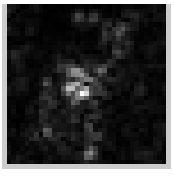

(b) N = 35 (scaled for display)

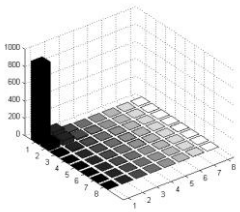

(c) GLCM plane, $d = 1$

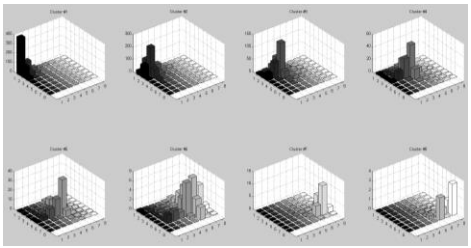

(d) FCOM planes, $d = 1$

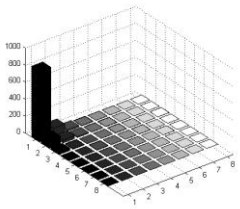

(e) GLCM plane, $d = 2$

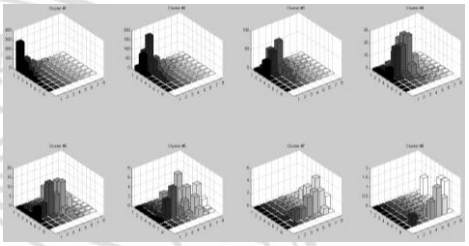

(f) FCOM planes, $d = 2$

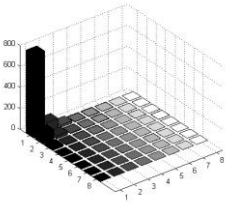

(g) GLCM plane, $d = 3$

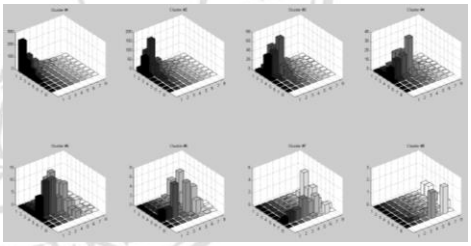

(h) FCOM planes, $d = 3$

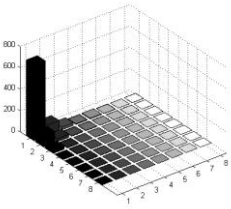

(i) GLCM plane, $d = 5$

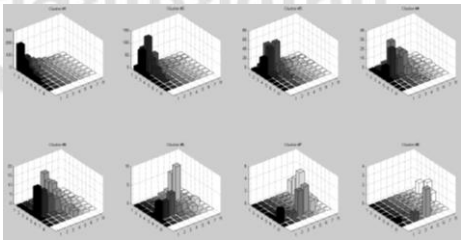

(j) FCOM planes, $d = 5$

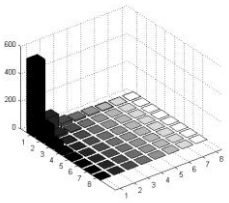

(k) GLCM plane, d = 10

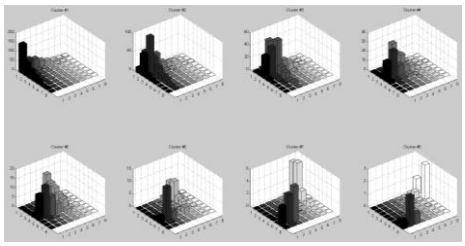

(l) FCOM planes, d = 10

Figure 6.7 (a) original BMP2 SAR image and (b) its corresponding sub-image (N = 35), the value of each FCOM planes for (c) d = 1, (d) d = 2, (e) d = 3, (f) d = 5, and (g) d = 10.

From the value of each GLCM and FCOM planes comparison in figure 6.7 for the same number of gray levels (or number of clusters), we can see that the GLCM planes were similar in all distances while FCOM planes with different d were very dissimilar. This will recognize the texture with low gay level distribution. In different gray levels, FCOM planes were also more information than the GLCM plane as shown in figure 6.8. In addition, the correct recognition rate was depended on the number of gray levels (N_g) for GLCM (or the number of clusters for FCOM) since in different gray levels makes the different values (or information) in FCOM planes.

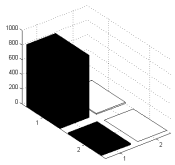

(a) GLCM plane (N_g = 2)

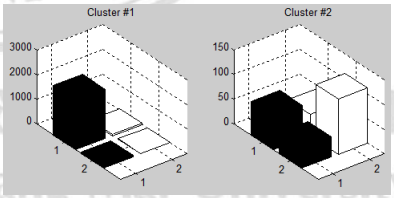

(b) FCOM planes (C = 2)

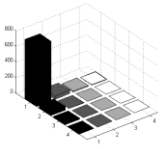

(c) GLCM plane (N_g = 4)

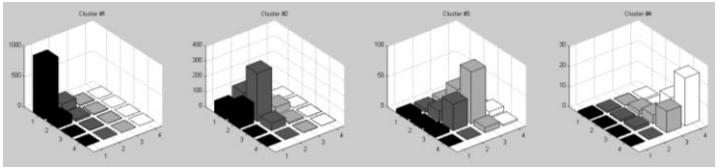

(d) FCOM planes (C = 4)

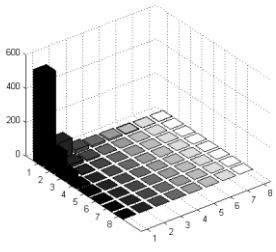

(e) GLCM plane (N_g = 8)

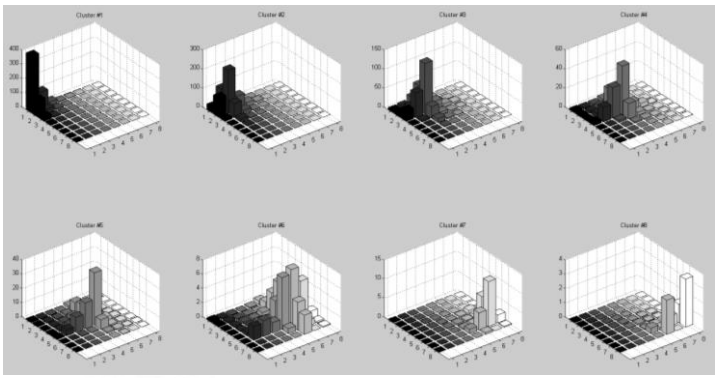

(f) FCOM planes (C = 8)

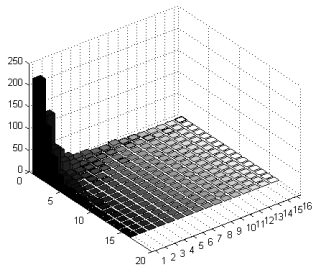

(g) GLCM plane (N_g = 16)

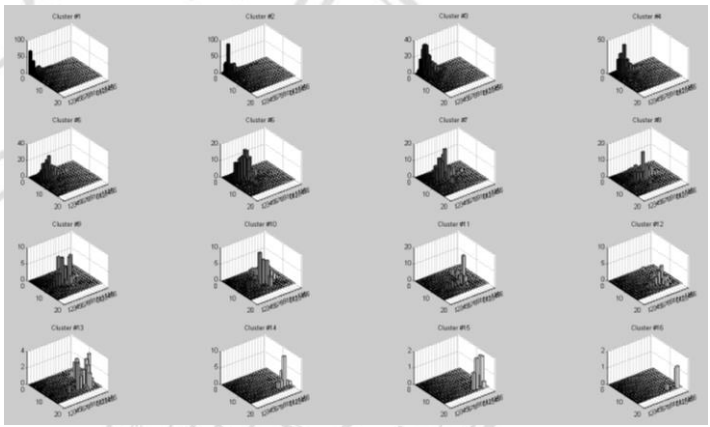

(h) FCOM planes (C = 16)

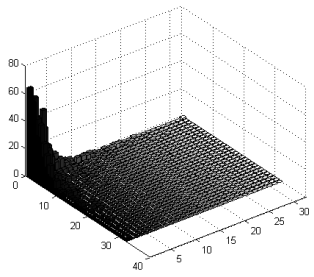

(i) GLCM plane (N_g = 32)

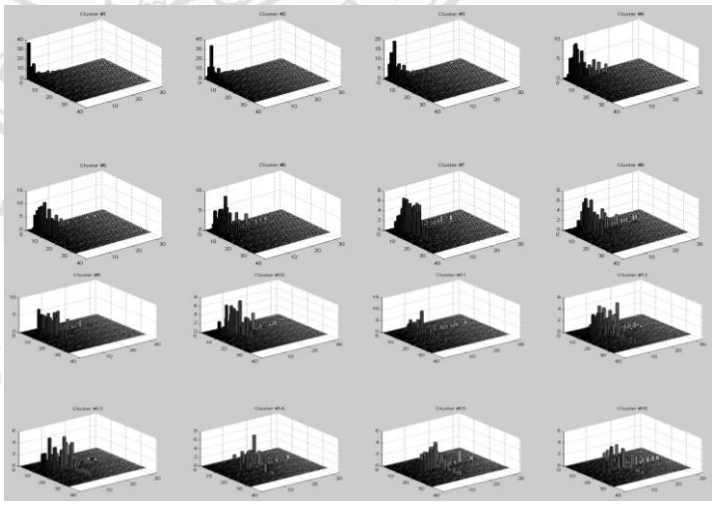

(j) FCOM planes (C = 32)

Figure 6.8 GLCM and FCOM planes where d = 10 and θ = 0° with different number of gray levels.

However, there were some miss recognition result images. The most incorrect classification occurred between APCs and Tank. BMP2 object look like rectangle shape with thin and long. They had more spot over image. BTR70 image had a square spot or circle spot somewhere. T72 was irregular shape with some spot. An example of similar FCOM planes between different objects is shown in figure 6.9.

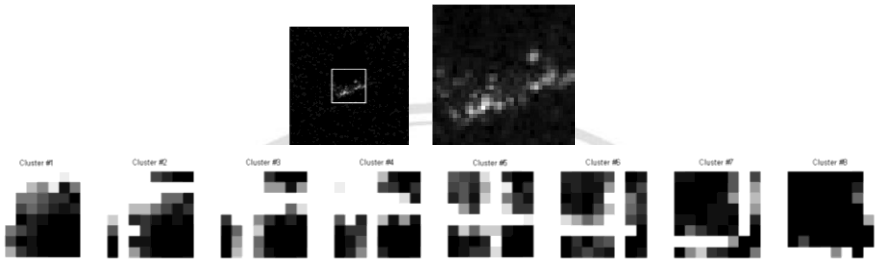

(a) Original BMP2 SAR image and coresponding FCOM planes

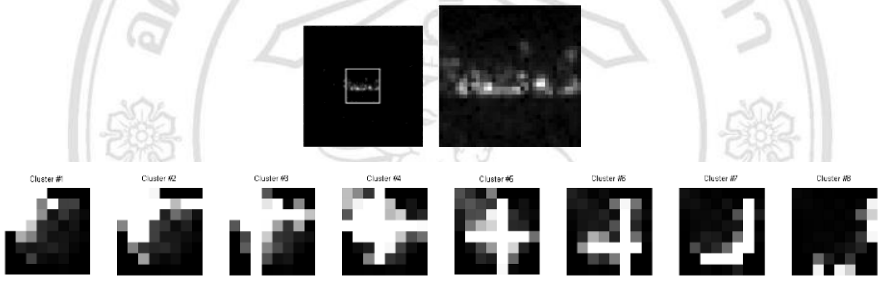

(b) Original BTR70 SAR image and coresponding FCOM planes

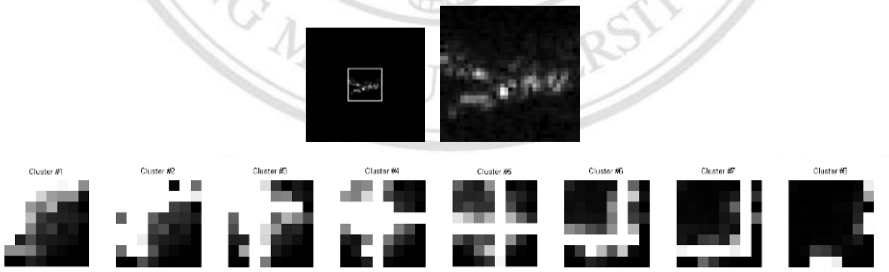

(c) Original T72 SAR image and coresponding FCOM planes

Figure 6.9 Example of similar FCOM planes between different objects.